Hierarchical Control of DC Coupled Fast EV Charging Station

Ali Sharida, *Member, IEEE*, Abdullah Berkay Bayindir, *Student Member, IEEE*, Sertac Bayhan, *Senior Member, IEEE*, and Haitham Abu-Rub, *Fellow, IEEE*

***Abstract*—This article proposes a new hierarchal control scheme for dc-coupled fast electric vehicle (EV) charging stations. This control scheme coordinates the charging activities of the linked EVs with renewable energy sources and external storage solutions. The proposed solution allows bidirectional power flow and provides various ancillary services to the grid. These services include low-voltage ride through (LVRT), high-voltage ride through, low-frequency ride through, high-frequency ride through, and voltage support (VS). To prove this concept, the article will focus on LVRT and VS services. In addition to the aforementioned objectives, the proposed scheme aims to minimize the power consumed from the ac grid and take the advantage of the available renewable energy, and harvest the maximum possible power from the available renewable resources. Experimental investigations are conducted to validate the proposed concept and prove its unique advantages.**

***Index Terms*—Ancillary services, dc coupled charging stations, fast electric vehicle (EV) charger, hierarchical control, renewable energies.**

I. Introduction

ELECTRIC vehicles (EVs) are game-changers for the automotive industry, ushering in a new era of environmentally friendly and sustainable transportation [1]. EVs are cleaner and more energy-efficient alternatives to conventional internal combustion engine vehicles. Although EVs hold great promise for a sustainable future, they also face several challenges that need to be addressed for widespread adoption. One of the key challenges is related to the charging process, including chargers' availability, charging time, and the impact on the grid.

Received 10 December 2024; revised 11 February 2025 and 14 March 2025; accepted 9 April 2025. Date of publication 14 April 2025; date of current version 26 May 2025. This work was supported in part by Qatar Research, Development and Innovation under Grant ARG01-0428-230023 and in part by the Gazi University Scientific Research Projects Coordination Unit under Grant FUI-2024-9556. Recommended for publication by Associate Editor H. Chung. *(Corresponding author: Ali Sharida.)*

Ali Sharida is with the Qatar Environmental and Energy Research Institute, Hamad Bin Khalifa University, Doha 34110, Qatar (e-mail: asharida@hbku.edu.qa).

Abdullah Berkay Bayindir is with Texas A&M University, College Station, TX 77840 USA, and also with Smart Grid Center, Texas A&M University at Qatar, Doha 23874, Qatar (e-mail: abdullah.bayindir@Qatar.tamu.edu).

Sertac Bayhan is with the Qatar Environmental and Energy Research Institute, Hamad Bin Khalifa University, Doha 34110, Qatar, and also with the Department of Electrical-Electronic Engineering, Technology Faculty, Gazi University, Ankara 06500, Türkiye (e-mail: sbayhan@hbku.edu.qa).

Haitham Abu-Rub is with Hamad Bin Khalifa University, Doha 34110, Qatar (e-mail: haburub@hbku.edu.qa).

Color versions of one or more figures in this article are available at https://doi.org/10.1109/TPEL.2025.3560343.

Digital Object Identifier 10.1109/TPEL.2025.3560343

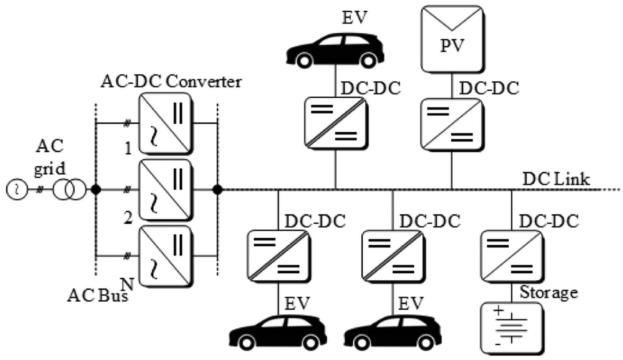

Fig. 1. DC link-coupled FEVC infrastructure.

These issues have drawn a lot of research attention in an effort to advance electrified transport to its next stage. A portion of these studies concentrated on the charging stations localization problem to address the issue of availability and minimize the impact of charging process on the grid [2], [3]. Other studies focused on reducing the cost and impact of increasing the number of charging stations [4], scalability aspects [5], and the reliability of power electronic systems [6].

Fast EV chargers (FEVCs) represent a ground-breaking advancement in the field of EVs. They offer a discernible increase in charging speed, can supply a substantial quantity of power to the EV's battery in a comparatively short period of time, in addition to possible grid support. Due to the advancement of bidirectional power converters, FEVCs are increasingly transforming from grid-stressors into relievers. They can be used as distributed storage systems, increase the inertia of the grid, enhance voltage and frequency stability of the grid, lowering peak demand, and improve the power factor and the quality of grid's power.

One of the best available infrastructures to achieve all of these objectives is the dc link-coupled FEVCs [5] shown in Fig. 1. In this infrastructure, multiple bidirectional ac–dc converters are connected in parallel to provide a common dc link. This simplifies the process of integrating photovoltaics (PVs) and storage systems. Moreover, such infrastructure reduces the number of the required converters, reduces the losses resulted from multi-stage power conversion, and enhances the scalability and flexibility of the charging system. To charge/discharge the EV, only single stage dc–dc converter is required to integrate the EV with the dc link.

This infrastructure attracted a global attention of research due to its unique benefits [7], [8]. Some of the researches proposed methods to integrate renewable energies such as PVs with bidirectional EV chargers [9], fuel-cells [10], and additional battery storage systems [11]. Another direction of research on dc link-coupled chargers is related to providing possible ancillary services such as supporting the voltage in dc microgrids [12] and enhancing the stability of ac grids [13]. Moreover, all ancillary services that can be implemented using the conventional FEVCs are applicable for the dc-link coupled chargers. However, these services are not well-addressed yet for this infrastructure, which performs one of the key motivations of this article.

Different than the conventional FEVC, which consists of only two cascaded converters, the main challenge of dc link-coupled FEVC infrastructure is the increased number of the effective components as this structure contains multiple EVs, multiple renewable energy resources, storage systems, and ac–dc converters. Therefore, these components must operate synchronously in a collaborated and coordinated manner to harvest the maximum possible benefits, services, and power quality. This triggers the necessity of a rigid hierarchal control technique that takes in considerations all available EVs, storage systems, renewable energies, ancillary services, and grid integration.

Hierarchal control techniques are widely spread in many applications especially in ac and dc microgrids. The main purpose of such control is to enable the intelligent and adaptable integration of distributed generation based on power electronics [14]. In general, the hierarchal control approach consists of three levels, namely tertiary control, secondary control, and primary control [1]. This approach shows multiple advantages for microgrids in terms of flexibility and holism. However, concerning EVs, there are numerous functionalities that are not combined in any other application. These functionalities include dc link formulation and regulation, vehicle to dc link, dc link to vehicle, charging profiles control, renewable energy to dc link flow control, dc link to grid, and grid to dc link.

Moreover, in EV charging application, the dc-link voltage regulation is the most challenging problem due to the intermittent nature of renewable energy sources, charging load variation, and the integration with the utility grid. Most of the papers share the regulation task among the available converters [15]. However, this method has many limitations as the SoC of the storage system is not guaranteed. Moreover, distributing the regulation among the available converters is very challenging in EV charging infrastructure as the number of EVs is not constant, they can suddenly connect or disconnect, and the users may accept or reject to participate in V2G services. These constraints were not studied in other papers.

In [16], a hierarchical control of power distribution in ultrafast charging station was presented. However, this method focuses solely on the primary and secondary control levels and does not discuss the tertiary level and how ancillary services can be integrated. Moreover, the integration with renewable energy and the effect of the intermittent nature of the renewable energies were not discussed.

To this end, this article proposes a new hierarchal control scheme for dc link coupled FEVCs as shown in Fig. 2. The proposed approach takes into consideration the existence of multiple EVs, renewable energies, and an external storage system. Moreover, the proposed solution can guarantee smooth power flow control between different EVs, renewable energies, and utility grid. In addition, the proposed strategy supports multiple grid services and provides enhanced EV charging functionalities.

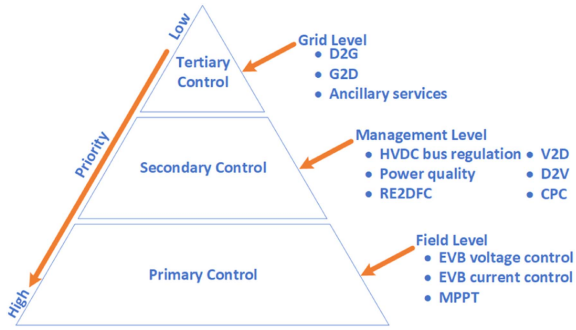

Fig. 2. The proposed hierarchical control approach for dc link coupled FEVCs.

The contributions of this article are summarized as follows,

1) A novel hierarchical control scheme for dc-coupled fast EV chargers.
2) A new control strategy is proposed for dc link regulation.
3) Optimal utilization of available dc power to enhance efficacy and reliability of the charging infrastructure.
4) Seamless integration of charging operations with grid ancillary services for enhanced grid support.
5) Smooth transition between grid-connected and islanded operation to improve system resilience and reliability.

II. System Description

A. AC–DC Converters

Fig. 3 illustrates the circuit diagram of the parallel AC–DC converters under consideration. The circuit consists of three active front-end rectifiers. All of them are bidirectional and have a common ac input (from utility grid) and a common dc output connected to dc link.

The dynamic model of these converters can be represented as follows [17]:

$$\mathbf{V}_{abc} = \sum_{i=1}^{3}\left[L_g\frac{d\mathbf{I}_{abci}}{dt} + R_{gi}\mathbf{I}_{abci} + \mathbf{U}_{abci}\right] \tag{1}$$

$$C\dot{V}_{dc} = 3\frac{V_dI_d + V_qI_q}{V_{dc}} - I_{dc} \tag{2}$$

where $\mathbf{U}_{abci} = [U_{ai} \quad U_{bi} \quad U_{ci}]^T$ represent the poles' voltages, $\mathbf{I}_{abci} = [I_{ai} \quad I_{bi} \quad I_{ci}]^T$ represent the grid currents, I_{dc} is the dc output/input current, V_d,V_q, I_d, and I_q refer to the grid voltages and currents in the synchronous dq frame, and $\mathbf{V}_{abc} = [V_a \quad V_b \quad V_c]^T$ is the grid voltage.

B. DC—DC Converters

Five bi-directional buck-boost converters are used to interface three EVs, PV, and a storage system to the dc link. The circuit

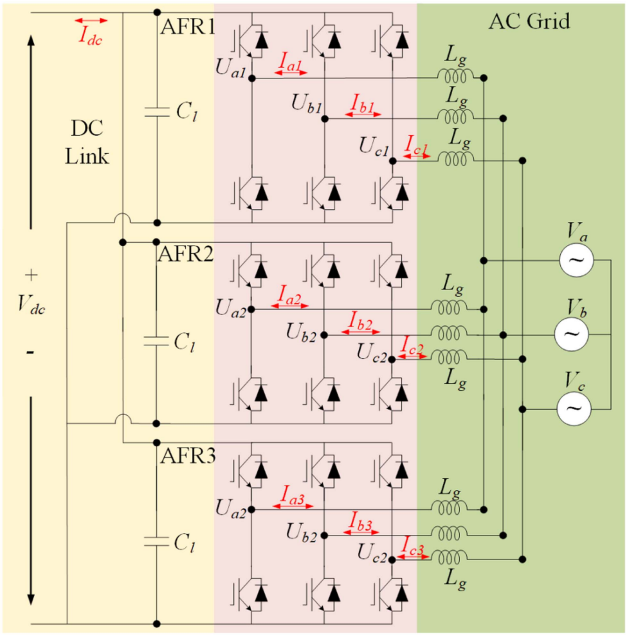

Fig. 3. Circuit diagram of the ac–dc converters.

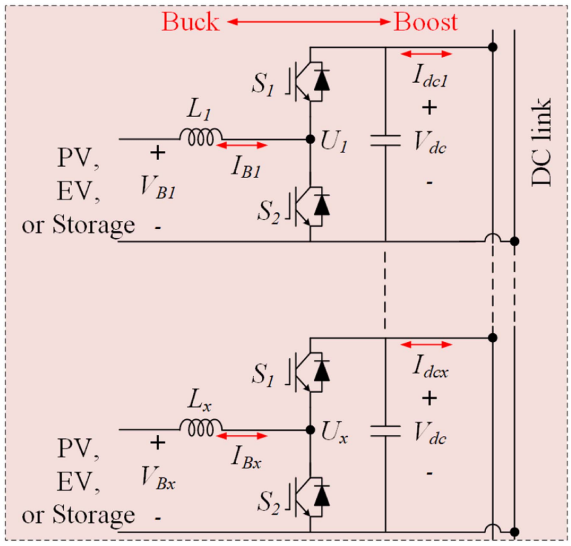

Fig. 4. Circuit diagram of the dc–dc converters.

diagram of the dc–dc converter is shown in Fig. 4. This converter operates in two modes, namely buck and boost. As a boost converter, it steps up the input voltage and supports the dc link. During this mode, the dynamic model of the converter is given by

$$\frac{dI_{Bx}}{dt} = \frac{1}{L_x}V_{Bx} - (1-U_x)\frac{1}{L_y}V_{\rm dc}$$
$$\frac{dV_{dc}}{dt} = (1-U_x)\frac{1}{C}I_{Bx} - \frac{1}{R_L C}V_{\rm dc} \quad (3)$$

where $x \in [1 \quad \dots \quad 5]$ represents the converter number, and U_x is the pole's voltage of the converter x, and V_{Bx}, I_{Bx}, *and* I_{dcx}

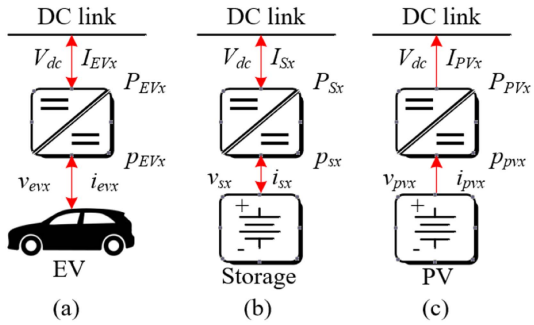

Fig. 5. Current, voltage, and power flow analysis. (a) EV analysis. (b) Storage system analysis. (d) PV system analysis.

are shown in Fig. 5. For the buck operation, the dynamic model is given by

$$\frac{dI_{Bx}}{dt} = \frac{1}{L_x}(U_x V_b - V_{\rm dc} - RI_{Bx})$$
$$\frac{dV_b}{dt} = \frac{1}{C}\left(I_{Bx} - \frac{V_{\rm dc}}{R_L}\right). \quad (4)$$

III. Primary Control Level

Primary control level represents the main control technique for each standalone converter in the system. In this level, each converter tries to achieve its primary objectives including regulating the output voltage and current.

A. *Primary Control for Battery-Connected DC Converters*

Charging process consists of two main intervals, constant current (CC) charging and constant voltage (CV) charging. CC charging starts at the beginning of the charging process when the EV sends its nominal power/current to the charger. The charger then keeps supplying a CC to EV battery until the state of charge (SoC) reaches 80%. At this instant, the charging mode is switched from CC to CV. The FEVC keeps monitoring the voltage of the EV battery and compares it to the nominal voltage, and based on the error of the voltage, a specific amount of current is delivered to the battery until it is fully charged.

It can be noticed that the dc converter is always acting as a controlled current source during the charging process. It is always receiving a reference current signal either from the EV during the CC charging mode or from the FEVC's voltage controller during the CV charging mode of operation. To this end, two controllers are required for the converter that works as FEVC, current controller and voltage controller. Although voltage controllers were extensively studied in the literature, the case is different for EVs. This is due to the high capacity of EVs' batteries, the time required to reach steady state is very long compared to other applications. Therefore, the proportional-integral controllers cannot be used as the integral term will integrate the error of the voltage for a very-long period which generates a huge accumulated integration error. Therefore, only the proportional controller is required as voltage regulator to generate the charging reference current signal during CV operation. As the current

controller is regulating the current during the entire charging process, modern and advanced controllers can be adopted to ensure that current converges to its reference value rapidly and smoothly. The selection of the control technique is based mainly on the type of the dc–dc converter. In this article, the sliding mode controller (SMC) is adopted due to its simplicity and robustness. The error between the reference and measured currents can be selected as a sliding surface

$$S_x = I_x^* - I_x \tag{5}$$

where x refers to x^{th} converter.

In fact, such selection of the sliding surface is useful in this case, because as S_x approaches zero, the current error approaches zero too, which is the goal of the control algorithm. Moreover, the control signal appears explicitly in the derivative of the sliding surface. To this end, the sliding surface can be used as a control law for the current regulation

$$U_{ix} = I_x^* - I_x. \tag{6}$$

During supplying CC to the EV's battery, its voltage increases gradually until the SoC reaches 80%. The voltage at this instant must be captured and stored to compute the optimal gain of the voltage controller. Otherwise, the charging current becomes unpredictable, it may have sudden increase or decrease. Moreover, to avoid any sudden current or voltage drop, seamless transition from CC to CV charging is an important aspect during the charging process. To achieve seamless transition, the following equality must be satisfied:

$$I_{Bx}^*\big|_{CC} = I_{Bx}^*\big|_{\text{SoC}=80\%} \tag{7}$$

where $I_{Bx}^*|_{CC}$ is the reference current during CC charging, and $I_{Bx}^*|_{\text{SoC}=80\%}$ is the current reference after the instant of switching to CV. (7) can be satisfied by selecting the proportional control gain (K_p) as follows:

$$K_p = \frac{I_{Bx}^*\big|_{CC}}{v_{ex}\big|_{\text{SoC}=80\%}} \tag{8}$$

where v_{ex} is error between the reference (nominal) voltage and the measured voltage and can be represented as

$$v_{ex} = V_{Bx}^* - V_{Bx}. \tag{9}$$

Finally, CV charging reference current can be described as shown in

$$I_{Bx}^*(v_e)\big|_{\text{CV}} = K_p\left(V_{Bx}^* - V_{Bx}\right). \tag{10}$$

B. Primary Control for PV Connected DC Converter

Due to the intermittent nature of PV systems, the primary control of PV converter must ensure stable and reliable integration with the dc link. Therefore, SMC-based current-controlled maximum power point tracking (MPPT) technique is employed for PV-connected dc converter.

At maximum power point, the system can be assumed to be at steady state, therefore the power delivered by the dc–dc converter to the load has the following properties:

$$\frac{dP_{\text{PV}}}{dt} = 0,$$
$$P_{\text{PV}} = I_{\text{PV}}V_{\text{PV}} \tag{11}$$

which gives the following result:

$$\frac{dI_{\text{PV}}}{dt} = 0. \tag{12}$$

Therefore, to design a current controller using SMC, the sliding surface can be chosen as shown

$$S_{\text{PV}} = I_{\text{PV}}^* - I_{\text{PV}}. \tag{13}$$

The PV current reference can be generated by using the incremental conductance MPPT technique [18]. It can be noticed from (13) that the sliding surface converges to zero as the error converges to zero, which represents the main objective of the controller. To this end, the current control law can be selected as the error of the current tracking as follows:

$$U_{\text{PV}} = I_{\text{PV}}^* - I_{\text{PV}}. \tag{14}$$

C. Primary Control of AC–DC Converters

In fact, many advanced, robust, and adaptive control techniques were proposed in the literature to control ac–dc converters [19]. Using SMC, the grid currents can be regulated depending on their power sharing ratios (R_i) as shown in

$$u_{ai} = I_{ai} - I_{ai}^*$$
$$u_{bi} = I_{bi} - I_{bi}^*$$
$$u_{ci} = I_{ci} - I_{ci}^* \tag{15}$$

where

$$I_{ai}^* = R_i I_d^* \cos(wt)$$
$$I_{bi}^* = R_i I_d^* \cos(wt + 2\pi/3)$$
$$I_{ci}^* = R_i I_d^* \cos(wt - 2\pi/3). \tag{16}$$

IV. Secondary Control Level

The main objective of secondary control level for dc coupled charging station is to create and regulate the dc-link voltage that connects and manages all elements. The major challenge to achieve this objective is the variety of the connected components, the wide range of scenarios and operating conditions, and the bidirectional power flow. As this infrastructure contains EVs, PVs, and an external storage system, a robust centralized controller must be designed that takes into account the role of each connected unit. In terms of possible scenarios and operating conditions, some of the EVs may need charging and other EVs are charged and can contribute to regulate the dc-link voltage. Another possible scenario when all the EVs require charging, or when all of them are charged and can inject power to the dc link. The PVs may or may not have the ability inject power to the dc bus, and the storage system may work as a load during charging or as a source during discharging. Finally, the challenge of power

flow direction is considered as the most challenging problem in this level.

AC-DC converters are usually responsible to form and regulate the dc-link bus, where they operate as rectifiers. In this case, the regulation process is easy as the main objective of any controlled rectifier is regulating the dc-link voltage. However, if the dc-link voltage contains surplus energy beyond what is required for charging the EVs, the excess power is converted into ac and is utilized to bolster the ac grid. In this scenario, the ac–dc converters function as inverters. In such case, the dc-link voltage serves as an input (uncontrolled state), hence regulating the dc voltage is not a primary objective. To this end, another converter should take the responsibility to regulate the dc-link voltage. However, the EVs are not qualified to achieve this goal as they can be connected or disconnected at any instance. The PV converter follows the maximum power point regardless the dc-link voltage level. Although the external storage converter is the most qualified device to achieve the dc-link voltage regulation, if the SoC goes beyond a specific level, the converter will not be able to achieve this functionality.

To deal with those challenges, this article proposes a novel control approach that utilizes the ac–dc converters to regulate the dc-link voltage regardless the direction of power flow. The basic principle of this control approach is to provide a feedforward current reference signal to the primary controller. This signal contains the total amount of power that should be consumed/injected from/to the dc-link to force the dc-link voltage to converge to its reference value. Therefore, it is worth analyzing the power, currents, and voltages of each device attached to the system.

Assuming that the efficiency of the dc converters approaches 100%, which makes the input power equals the output power

$$\begin{aligned} P_{\mathrm{EV}x} &= p_{evx} \\ P_{Sx} &= p_{sx} \\ P_{\mathrm{PV}x} &= p_{pvx}. \end{aligned} \tag{17}$$

Substituting the currents and voltages of all components into (17) shows the detailed relation between the currents and voltages of the connected devices with the dc-link voltage as shown in Fig. 5

$$\begin{aligned} V_{\mathrm{dc}} I_{\mathrm{EV}x} &= v_{evx} i_{evx} \\ V_{\mathrm{dc}} I_{Sx} &= v_{sx} i_{sx} \\ V_{\mathrm{dc}} I_{PVx} &= v_{pvx} i_{pvx}. \end{aligned} \tag{18}$$

The current through the dc-link voltage can be described as follows:

$$I_{dc} = \sum_{x=1}^{E} I_{\mathrm{EV}x} + \sum_{x=1}^{S} I_{Sx} + \sum_{x=1}^{P} I_{\mathrm{PV}x} \tag{19}$$

where E is the number of EVs, S is the number of storage systems, and P is the number of PVs.

Substituting (18) into (19), leads to compute the total current flowing through the dc link

$$I_{\mathrm{dc}} = \sum_{x=1}^{E} \frac{v_{evx} i_{evx}}{V_{\mathrm{dc}}} + \sum_{x=1}^{S} \frac{v_{sx} i_{sx}}{V_{\mathrm{dc}}} + \sum_{x=1}^{P} \frac{v_{pvx} i_{pvx}}{V_{\mathrm{dc}}}. \tag{20}$$

Similar analysis can be done for the ac side, the apparent power (S_g) can be written as follows:

$$S_g = \sqrt{3} V_{g\_\mathrm{rms}} I_{g\_\mathrm{rms}} \tag{21}$$

where V_{g_rms} and I_{g_rms} are the rms grid voltage and grid current, respectively. Assuming a lossless ac-dc conversion, the relation between ac side and dc side is described as follows:

$$\sqrt{3} V_{g\_\mathrm{rms}} I_{g\_\mathrm{rms}} = V_{\mathrm{dc}} I_{\mathrm{dc}}. \tag{22}$$

To this end, the I_{g_rms} that is required to be consumed/injected from/into the grid to maintain a CV is described as follows:

$$I^*_{g\_\mathrm{rms}} = \frac{V^*_{\mathrm{dc}}}{\sqrt{3} V_{g\_\mathrm{rms}}} \left[\sum_{x=1}^{E} I_{\mathrm{EV}x} + \sum_{x=1}^{S} I_{Sx} + \sum_{x=1}^{P} I_{\mathrm{PV}x} \right]. \tag{23}$$

Equation (23) is formulated based on the assumption of 100% efficiency for all converters. However, this is not true, as each converter has losses which increase the dc-link voltage tracking error. Hence, an integral voltage feedback term is added to (23) to overcome this problem

$$\begin{aligned} I^*_{g\_\mathrm{rms}} = \frac{V^*_{\mathrm{dc}}}{\sqrt{3} V_{g\_\mathrm{rms}}} & \left[\sum_{x=1}^{E} I_{\mathrm{EV}x} + \sum_{x=1}^{S} I_{Sx} + \sum_{x=1}^{P} I_{\mathrm{PV}x} \right] \\ & + K_i \int (V^*_{\mathrm{dc}} - V_{\mathrm{dc}}) dt. \end{aligned} \tag{24}$$

The use of (24) to generate a reference current signal for the ac–dc converters ensures the following.

1) Accurate regulation of the dc-link voltage regardless of the amount of losses.
2) Taking into consideration the direction of the power flow for each element. For example, if one of the EVs is charging, its current will be negative. This will reduce the dc available power, which automatically decreases the amount of power injected to the grid.
3) Allows the ac–dc converters to regulate the dc-link voltage regardless the direction of power flow. If the dc power is positive, this means that $I^*_{g\_\mathrm{rms}}$ is positive too. This leads to inject positive current into the grid. Otherwise, if the dc available power is less than the required (i.e., all EVs are charging), the available dc power will be negative, then $I^*_{g\_\mathrm{rms}}$ will be negative too. This means that $I^*_{g\_\mathrm{rms}}$ is being consumed from the grid.
4) Optimal power consumption/injection from the grid. Assuming that the available dc power is equal to the required dc power, then $I^*_{g\_\mathrm{rms}}$ equals to 0. In such case, all the available dc power will be utilized without the need of the ac grid. If the available power becomes slightly larger than the required, then the remaining power will be injected to the grid. Finally, if the available power is less than the required, then all available power will be utilized and the remaining will be consumed from the grid.

Moreover, this method enables the exact knowledge of the available power which simplifies the control process of ancillary services as $I^*_{g\_\mathrm{rms}}$ can be easily converted into active and reactive current references based on the type of ancillary service.

V. Tertiary Control Level

The main objectives of the tertiary control level are power flow control, energy management, and economic dispatch. Energy management systems were extensively studied in the literature, while economic dispatch is out of scope of this article. Therefore, this section will focus on the power flow control between the ac grid and the dc-link voltage. Although the amount of power flow is shown in (24), more details are required about how the power will be injected to the grid or to the dc link, and how to distribute the available power on the active and reactive components of the injected currents. All of these aspects depend on the type of the service that is utilized to support the grid. There are numerous methods to support the grid including low-voltage ride through (LVRT), high-voltage ride through, low-frequency ride through, high-frequency ride through, and voltage support. While the proposed system has the ability to provide all of the mentioned grid ancillary services, only LVRT and VS is being discussed for the sake of length.

LVRT refers to system's capacity to withstand voltage sags over a specified time frame, as depicted in Fig. 6(a) for various country codes [20]. Voltage sags in utility grids commonly arises from the changes in connected inductive loads. The capability FEVC infrastructure to inject reactive power into the grid becomes essential for grids' stability in such scenarios. This capability allows the linked EVs to contribute to grid stability through the use of the FEVC infrastructure, next to their roles in charging functionalities.

Although there is no LVRT standards for the proposed FEVC infrastructure, the adoption of the German grid code for LVRT operations establishes a standardized guideline. The German grid code requirement states that for every 1% of voltage drop at the point of common coupling, 2% of the rated current must be injected as reactive into the grid as shown in Fig. 6(b). Beyond a 50% voltage drop, only reactive current injection is required for a maximum of 1 s [21]. This relation can be described as following:

$$I^*_q = \begin{cases} 0 & 0.9 < v_{\mathrm{p.u.}} \leq 1.0 \\ 2\left(1 - v_{\mathrm{p.u.}}\right) I_n & 0.5 < v_{\mathrm{p.u.}} \leq 0.9 \\ I_n & 0 < v_{\mathrm{p.u.}} \leq 0.5 \end{cases} \tag{25}$$

where I^*_q is the reactive current reference, $v_{\mathrm{p.u}}$ is the grid voltage per unit, and I_n is the nominal current of the system.

Equation (25) shows that no reactive power injection is needed for LVRT if the voltage drop is less than 10%. However, for voltage stability issues, it is recommended to enable a static-voltage support technique in this scenario. Static voltage support depends on injecting reactive power proportional to the voltage drop. Therefore, when the voltage drop is less than 10%, reactive current reference is generated based on the type of ancillary service such as voltage support.

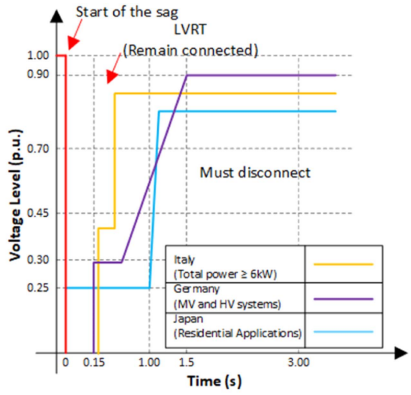

(a)

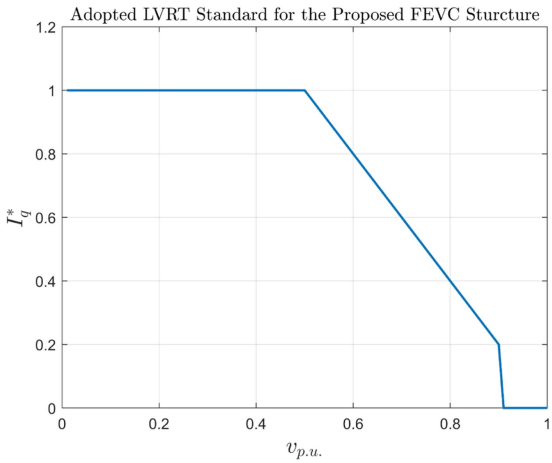

(b)

Fig. 6. LVRT standards.(a) Timing standards. (b) Reactive current support.

After computing I^*_q, I^*_d can be derived as follows:

$$\underbrace{\left(\sqrt{3} I^*_{\mathrm{g\_rms}} V_{g\_\mathrm{rms}}\right)}_{S} = \sqrt{\underbrace{\left(\frac{3 V_d I^*_d}{2}\right)^2}_{P} + \underbrace{\left(\frac{3 V_d I^*_q}{2}\right)^2}_{Q}} \tag{26}$$

where $V_{\mathrm{g\_rms}}$ and V_d are the rms and direct component of the grid voltage. Therefore, the I^*_d can be calculated as follows:

$$I^*_d = \sqrt{\left(\frac{2\sqrt{3} I^*_{g\_\mathrm{rms}} V_{g\_\mathrm{rms}}}{3 V_d}\right)^2 - \left(I^*_q\right)^2}. \tag{27}$$

After the computation of I^*_q and I^*_d components, tertiary control passes the $\mathbf{I}^*_{dq}$ variable to the secondary control level, as illustrated in Fig. 7.

Although the standards mentioned in this article do not specifically address the FEVC infrastructure, it is currently more common to encounter distributed energy resources on distribution networks. Therefore, this code is applicable to EVs that are considered distributed energy resources or storage systems.

VI. Expiremental Results

To validate the proposed hierarchal control approach, a lab-scale testbed was built as shown in Fig. 8. The testbed includes

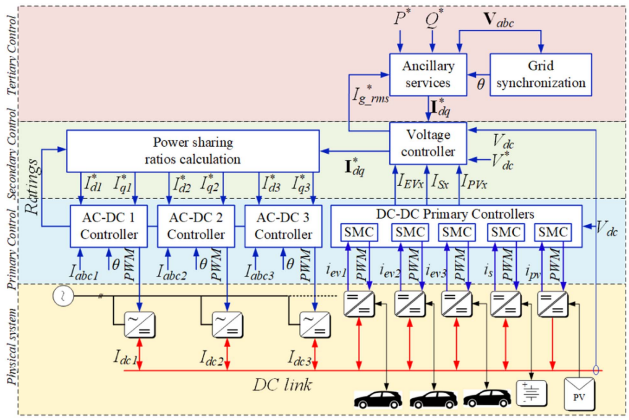

Fig. 7. Proposed hierarchal control block diagram.

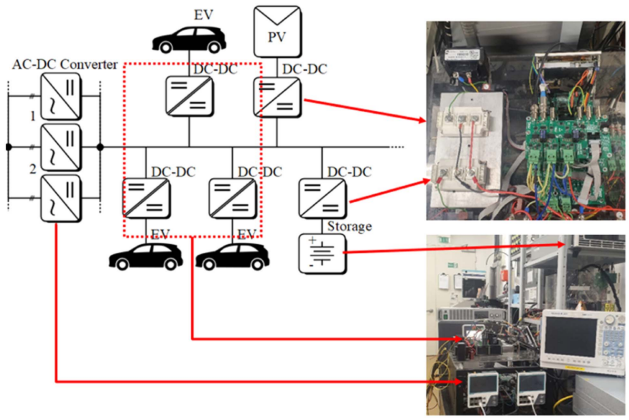

Fig. 8. Experimental testbed for dc coupled EV charging station.

TABLE I
EXPERIMENTAL PARAMETERS

Name	*Symbol*	*Value*
DC link voltage	V_{dc}	400V
EV nominal voltage	V_{EV}	400V
Name	***Symbol***	***Value***
Initial battery voltage	V_{EV0}	360V
Initial SoC	SoC_0	20%
Storage nominal voltage	V_S	400V
AC Grid voltage	V_{abc}	110 V_{rms}
Battery nominal capacity	C_n	1AH
Rated power for each converter	P_{rated}	4KW

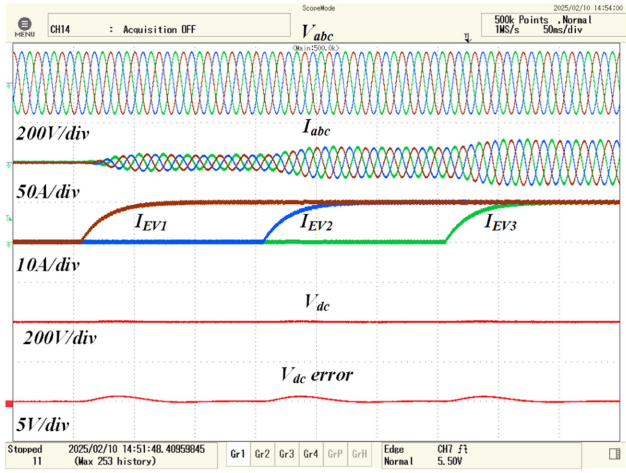

Fig. 9. Response during injecting real power from the dc link to the ac grid.

three EVs, which are emulated by Cinergia bidirectional ac/dc grid emulator, which consists of three-independent batteries emulator. The external storage system is implemented using Chroma 62000D, the PV is emulated using RE-005 PV-Emulator power supply, and the utility grid is emulated using California Instruments MX-30 regenerative grid emulator. All parameters used in this setup are given in Table I. It is worth noting that the capacity of the batteries is selected very low (1Ah) to make the charging time short to present the full charging profile in a single figure.

A. Injecting Power to the Grid

When the first EV is ready to inject power, the power starts flowing from the dc link to the utility grid.

As more EVs contribute, the power injected into the ac grid increases, as demonstrated in Fig. 9. It can be noticed from this experiment that the ac–dc converters have succeeded to regulate the dc-link voltage even if they are working as inverters, regardless the amount of the injected power, the number of EVs, and the availability of renewable energies. Moreover, the dc-link voltage is well-regulated with ripples at transient not exceeding 2%, and the grid currents are sinusoidal and in-phase with the grid voltages, which means the power factor is unity. It is worth noting that there is 180° phase shift between the voltage and current, which means the current is negative and being consumed from the dc link and injected to the ac grid.

B. Charging the EVs From the Utility Grid

In this mode, all ac–dc converters function as rectifiers, transferring power from the utility grid to the dc link. This power injection is directly proportional to the number of connected EVs and their rated power, while inversely proportional to the available power from renewable resources. The grid's response and the dc-link voltage in this case are illustrated in Fig. 10 for one, two, and three EVs during the charging mode. Similar to the previous case, the dc-link voltage is well-regulated regardless the direction of power flow, and the grid current is well regulated.

C. Integration With PV and Storage System

The experiments in this section start with no EVs connected to the dc bus, the PV is connected, and the SoC of the storage system is 75%. Therefore, the power generated from the PV is used to charge the battery storage as shown in Fig. 11. As

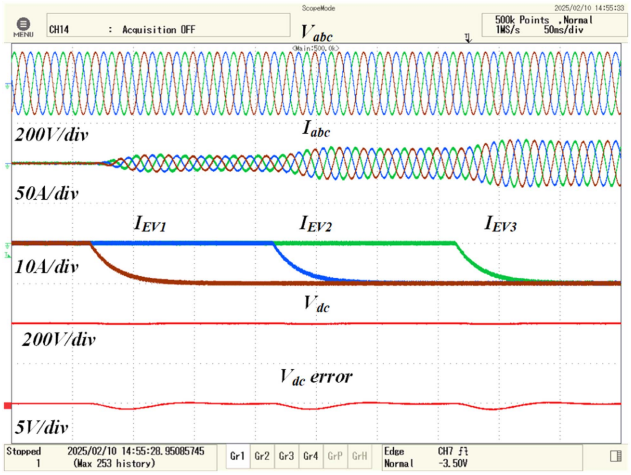

Fig. 10. Response during EVs charging.

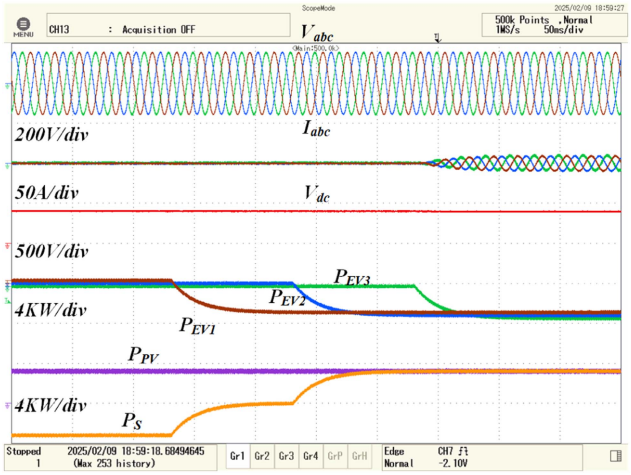

Fig. 11. Experimental response of the charging system while connecting the EVs while integrating PV and storage system.

the first EV is connected, the PV power is sufficient to charge the EV alone, so the power of the storage system converges to zero. Once the second EV is connected, the storage system starts to contribute to the charging process making the net power equals zero. Once the third EV is connected, the power from the PV and the storage becomes insufficient, so the remaining power is consumed from the grid. This experiment shows the smooth regulation of the dc-link voltage, the power of each terminal device, and the grid current. Moreover, it shows how the power consumed from the grid is always minimized, while the available renewable energy is fully utilized. In addition, it shows the robustness of the proposed control approach to regulate the dc-link voltage during steady state and transient operations.

After all EVs are connected, an intentional shading is applied to the PV as shown in Fig. 12. In Fig. 12(a), the maximum power point of the PV is dropped by 50% to emulate the partial shading of the PV, while in Fig. 12(b) the drop is 100% to emulate the full shading scenario. In both cases, the required power is consumed from the grid, which maintains a constant dc-link voltage and a

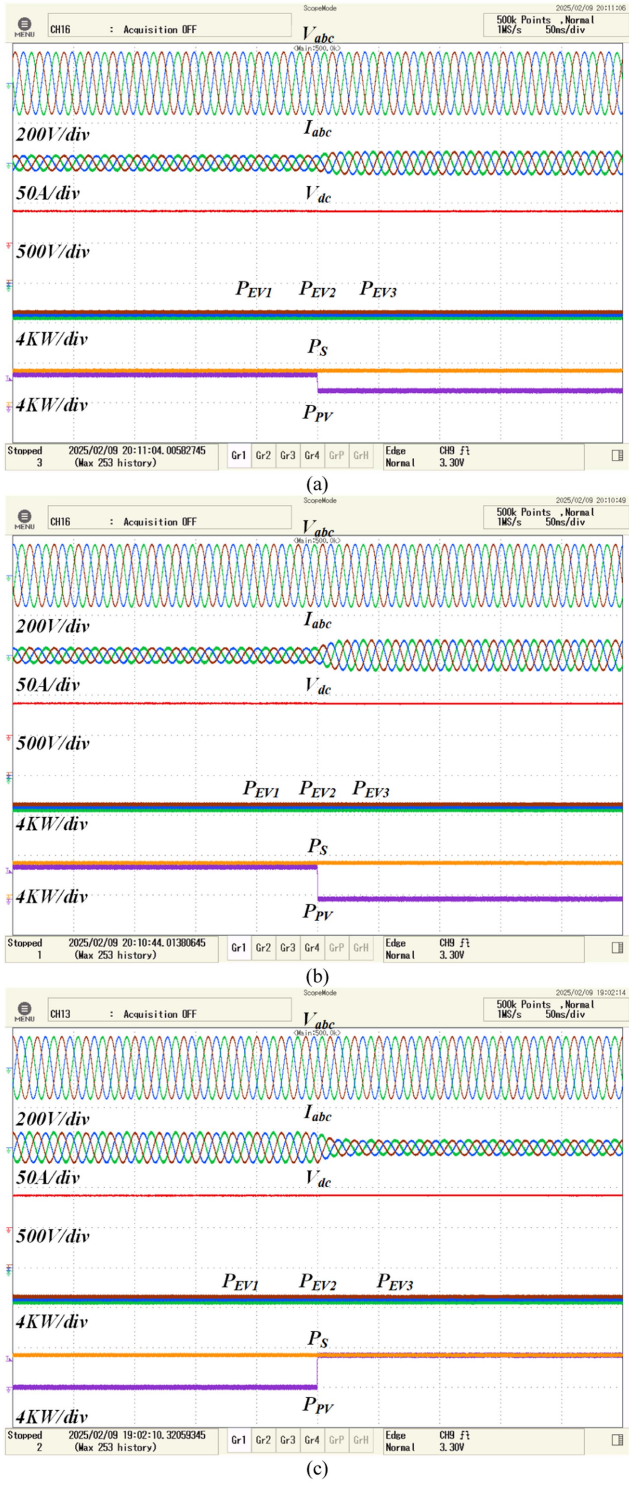

Fig. 12. Experimental response of the charging system during sudden shading. (a) 50%. (b) 100%. (c) No shading.

constant charging power on the EVs side. Similarly, when the shading is finished, the power of the PV is fully utilized and the power from the grid is minimized as shown in Fig. 12(c). It can be noticed that the power is compensated smoothly from the grid side with no ripples or overshoot which ensures the robustness

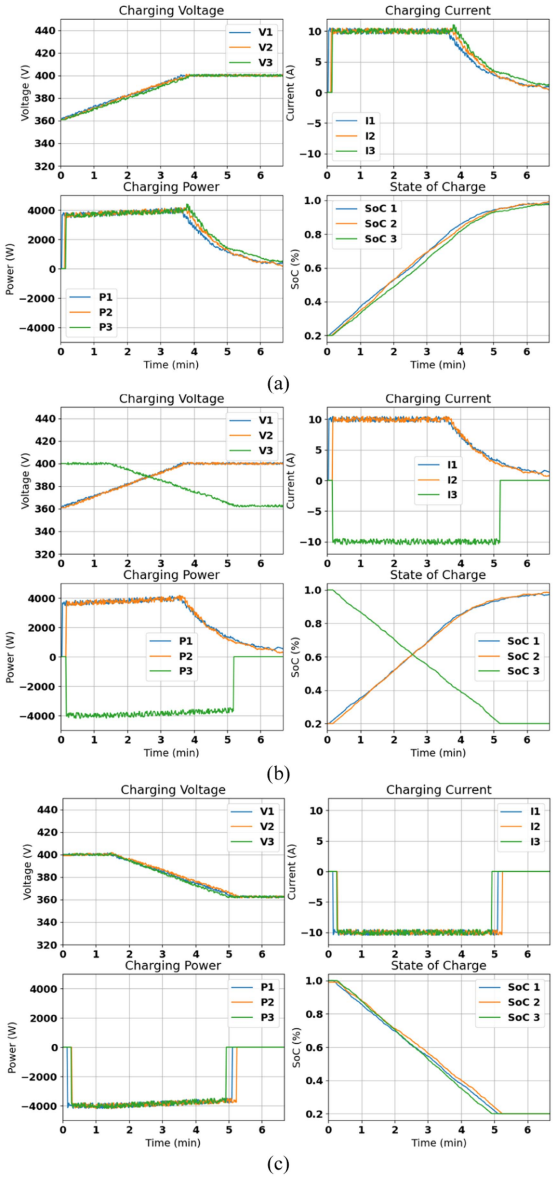

Fig. 13. Complete charging profiles. (a) All EVs are charging. (b) Two EVs are charging, and one is discharging. (c) All EVs are discharging.

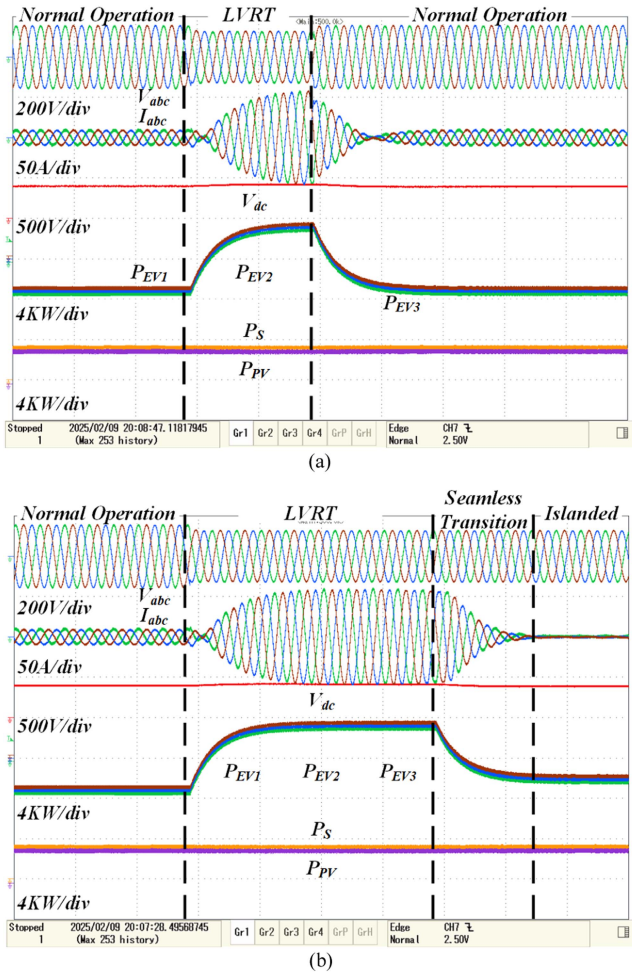

Fig. 14. LVRT response. (a) Voltage is restored within LVRT interval. (b) Voltage is not restored and islanded operation is enabled.

of the proposed approach against the intermittent nature of the RES's.

D. Charging Profiles

In this section, the charging profile of each EV is shown for all possible scenarios. The data for these charging profiles are exported from the battery emulator during the experiments and then plotted using Python language. The charging profiles are depicted in Fig. 13 as follows. In Fig. 13(a), all EVs are in charging mode. Here, all available renewable energies are utilized to charge the EVs, with any additional power required being drawn from the utility grid. In Fig. 13(b), some EVs are charging while others are discharging. The power of the discharging EVs and the available renewable energy are utilized for the charging EVs. In this case, the ac–dc converters may work as inverters or rectifiers based on the difference between the available and required dc power. Finally, in Fig. 12(c), all EVs are in discharging mode. If the storage system can store extra power, the power injected from EVs will be used to charge the storage system, otherwise, it will be injected to the grid.

E. Low Voltage Ride Through and Voltage Support

To show the ability of the proposed control approach to achieve ancillary services, LVRT and voltage support functionalities are validated as shown in Fig. 14. The voltage of the grid intentionally sags around 20% from its nominal voltage, and the EV transition from charging to discharging mode smoothly to support the grid. In Fig. 14(a), the voltage is restored before the end of LVRT period, so the EVs transition to normal operation. However, in Fig. 14(b), the voltage is not restored withing the LVRT interval, so the EVs start the seamless transition to islanded operation. In this mode, the EVs will utilize the available power from PV and storage without using any power from the grid.

Therefore, the power from the PV and the storage (8 KW total) are distributed equally among the three EVs (2.67 KW

each). This test shows the ability of the proposed approach to seamlessly transition between rectification operation, grid support operation, and islanded operation. In all cases, the power, current, and the dc-link voltage are regulated smoothly and effectively to eliminate the effects of power flow changes.

VII. Conclusion

A new hierarchal control approach was proposed in this article for dc-coupled fast EV chargers. All control levels (primary, secondary, and tertiary) were discussed, analyzed, and validated experimentally. The proposed approach was designed with the objective of integrating ac grid, renewable energies, and external storage systems with the charging infrastructure. The proposed approach was able to perform all charging requirements and provide multiple ancillary services to the grid. One of the key advantages of the proposed hierarchal control strategy is scalability and flexibility. The methodology provides high scalability and flexibility to add or integrate any additional component (including renewable energies, storage systems, dc loads, etc.) to the infrastructure. Similarly, energy management systems and load management strategies can be easily integrated.

Acknowledgment

The statements made herein are solely the responsibility of the authors.

References

[1] S. S. Refaat, O. Ellabban, S. Bayhan, H. Abu-Rub, F. Blaabjerg, and M. M. Begovic, *Smart Grid and Enabling Technologies*. Hoboken, NJ, USA: Wiley, 2021.

[2] I. S. Bayram, U. Zafar, and S. Bayhan, "Could petrol stations play a key role in transportation electrification? A GIS-based coverage maximization of fast EV chargers in urban environment," *IEEE Access*, vol. 10, pp. 17318–17329, 2022.

[3] Y. Zhang, J. Chen, L. Cai, and J. Pan, "Expanding EV charging networks considering transportation pattern and power supply limit," *IEEE Trans. Smart Grid*, vol. 10, no. 6, pp. 6332–6342, Nov. 2019.

[4] P. Chatterjee and M. Hermwille, "Tackling the challenges of electric vehicle fast charging," *ATZelectronics Worldwide*, vol. 15, no. 10, pp. 18–22, 2020.

[5] A. Sharida, S. Bayhan, and H. Abu-Rub, "Enhancing scalability of fast electric vehicle charging stations: Solutions for AC-DC side integration and regulation," *IEEE Open J. Ind. Electron. Soc.*, vol. 4, pp. 720–731, 2023.

[6] F. Blaabjerg, H. Wang, I. Vernica, B. Liu, and P. Davari, "Reliability of power electronic systems for EV/HEV applications," *Proc. IEEE*, vol. 109, no. 6, pp. 1060–1076, Jun. 2021.

[7] H. Tu, H. Feng, S. Srdic, and S. Lukic, "Extreme fast charging of electric vehicles: A technology overview," *IEEE Trans. Transp. Electrific.*, vol. 5, no. 4, pp. 861–878, Dec. 2019.

[8] N. Deb, R. Singh, R. R. Brooks, and K. Bai, "A review of extremely fast charging stations for electric vehicles," *Energies*, vol. 14, no. 22, 2021, Art. no. 7566.

[9] A. Verma, B. Singh, A. Chandra, and K. Al-Haddad, "An implementation of solar PV array based multifunctional EV charger," *IEEE Trans. Ind. Appl.*, vol. 56, no. 4, pp. 4166–4178, Jul./Aug. 2020.

[10] M. Patterson, N. F. Macia, and A. M. Kannan, "Hybrid microgrid model based on solar photovoltaic battery fuel cell system for intermittent load applications," *IEEE Trans. Energy Convers.*, vol. 30, no. 1, pp. 359–366, Mar. 2015.

[11] W. Vermeer, G. R. C. Mouli, and P. Bauer, "Optimal sizing and control of a PV-EV-BES charging system including primary frequency control and component degradation," *IEEE Open J. Ind. Electron. Soc.*, vol. 3, pp. 236–251, 2022.

[12] N. Poursafar, S. Taghizadeh, M. J. Hossain, and M. Karimi-Ghartemani, "A voltage-supportive controller for ultra-fast electric vehicle chargers in islanded DC microgrids," *J. Modern Power Syst. Clean Energy*, vol. 11, no. 3, pp. 896–906, May 2023.

[13] F. Mandrile, D. Cittanti, V. Mallemaci, and R. Bojoi, "Electric vehicle ultra-fast battery chargers: A boost for power system stability?," *World Elect. Veh. J.*, vol. 12, no. 1, 2021, Art. no. 16.

[14] I. Poonahela et al., "Hierarchical model-predictive droop control for voltage and frequency restoration in AC microgrids," *IEEE Open J. Ind. Electron. Soc.*, vol. 4, pp. 85–97, 2023.

[15] Y. Dou, M. Chi, Z.-W. Liu, G. Wen, and Q. Sun, "Distributed secondary control for voltage regulation and optimal power sharing in DC microgrids," *IEEE Trans. Control Syst. Technol.*, vol. 30, no. 6, pp. 2561–2572, Nov. 2022.

[16] A. Blanch-Fortuna, D. Zambrano-Prada, O. López-Santos, A. E. Aroudi, L. Vázquez-Seisdedos, and L. Martinez-Salamero, "Hierarchical control of power distribution in the hybrid energy storage system of an ultrafast charging station for electric vehicles," *Energies*, vol. 17, no. 6, 2024, Art. no. 1393.

[17] A. Sharida, N. Kamal, H. Alnuweiri, S. Bayhan, and H. Abu-Rub, "Digital twin-based diagnosis and tolerant control of t-type three-level rectifiers," *IEEE Open J. Ind. Electron. Soc.*, vol. 4, pp. 230–241, 2023.

[18] M. H. Ibrahim, S. P. Ang, M. N. Dani, M. I. Rahman, R. Petra, and S. M. Sulthan, "Optimizing step-size of perturb & observe and incremental conductance MPPT techniques using PSO for grid-tied PV system," *IEEE Access*, vol. 11, pp. 13079–13090, 2023.

[19] S. Bayhan and H. Komurcugil, "Sliding-mode control strategy for three-phase three-level T-type rectifiers with DC capacitor voltage balancing," *IEEE Access*, vol. 8, pp. 64555–64564, 2020.

[20] D. J. Rincon, M. A. Mantilla, J. M. Rey, M. Garnica, and D. Guilbert, "An overview of flexible current control strategies applied to LVRT capability for grid-connected inverters," *Energies*, vol. 16, no. 3, 2023, Art. no. 1052.

[21] S. Xu, Y. Xue, and L. Chang, "Review of power system support functions for inverter-based distributed energy resources-standards, control algorithms, and trends," *IEEE Open J. Power Electron.*, vol. 2, pp. 88–105, 2021.

Ali Sharida (Member, IEEE) received the B.E. degree in mechatronics engineering from Palestine Technical University, Tulkarm, Palestine, in 2013, the M.Sc. degree in mechatronics engineering from Palestine Polytechnic University, Hebron, Palestine, in 2020, and the Ph.D. degree in electrical engineering from Texas A&M University, College Station, TX, US, in 2024.

In 2022, he was an Associate Research Assistant with Texas A&M University at Qatar. He is currently a Postdoctoral Researcher with the Qatar Environment and Energy Research Institute, Hamad Bin Khalifa University, Ar-Rayyan, Qatar. His research focuses on energy management systems, demand response algorithms, smart charging technologies, system identification, power converters, and adaptive control.

Abdullah Berkay Bayindir (Student Member, IEEE) received the B.Sc. degree in electrical and electronics engineering from TOBB Economy and Technology University, Ankara, Türkiye, in 2023. He is currently working toward the Ph.D. degree in grid ancillary services with Texas A&M University, College Station, TX, USA.

His research interests include power converters, advanced control, renewable energy, and embedded software programming.

Sertac Bayhan (Senior Member, IEEE) received the M.S. and Ph.D. degrees in electrical engineering in 2008 and 2012, respectively, from Gazi University, Ankara, Türkiye, where he is graduated as valedictorian.

He has acquired $13M in research funding and authored or coauthored more than 170 papers in mostly prestigious IEEE journals and conferences. He is also the coauthor of three books and six book chapters. His research encompasses power electronics and their applications in next-generation power and energy systems, including renewable energy integration, electrified transportation, and demand-side management.

Dr. Bayhan is currently an Associate Editor for TRANSACTIONS ON INDUSTRIAL ELECTRONICS, IEEE JOURNAL OF EMERGING AND SELECTED TOPICS IN INDUSTRIAL ELECTRONICS, IEEE OPEN JOURNAL OF THE INDUSTRIAL ELECTRONICS SOCIETY, and IEEE INDUSTRIAL ELECTRONICS TECHNOLOGY NEWS, and a Guest Editor for IEEE TRANSACTIONS ON INDUSTRIAL INFORMATICS.

Haitham Abu-Rub (Fellow, IEEE) received the M.Sc. degree from Gdynia Maritime Academy, Gdynia, Poland, 1990, and the Ph. D. degree from Technical University of Gdansk, Poland, in 1995, all in electrical engineering, and also another Ph.D. degree from Gdansk University, Gdansk, Poland, in 2004, in humanities.

Since 2006, he has been with Texas A&M University at Qatar, Doha, Qatar, where he is currently a Professor and the Managing Director of the Smart Grid Center Extension. He has co-authored more than 550 journal and conference papers, six books, and six book chapters. His main research interests are energy conversion systems, smart grid, renewable energy systems, electric drives, and power electronic converters.

Dr. Abu-Rub is the recipient of many prestigious national and international awards and recognitions, such as the American Fulbright Scholarship and the German Alexander von Humboldt Fellowship. Dr. Abu-Rub is the Co-Editor in Chief for IEEE TRANSACTIONS ON INDUSTRIAL ELECTRONICS.